

Influences of indium doping and annealing on microstructure and optical properties of cadmium oxide thin films

Yuankun Zhu¹ · Pei Lei² · Jiaqi Zhu² · Jiecai Han²

Received: 30 July 2015 / Accepted: 30 November 2015 / Published online: 17 March 2016
© Springer-Verlag Berlin Heidelberg 2016

Abstract The influences of indium doping and subsequent annealing in nitrogen and air atmospheres on the microstructure and optical properties of cadmium oxide films were studied in detail with the aid of various characterizations. X-ray photoelectronic spectroscopy analysis shows that indium atom forms chemically oxidized bonds in Cd–O matrix. X-ray diffraction results demonstrate that CdO structure remains FCC structure with indium doping, whereas the preferential orientation transforms from (222) into (200) orientation. Indium doping prevents the large crystalline growth, and this role still works under both nitrogen and air annealing processes. Similarly, CdO films show rough surface under annealing conditions, but the force has been greatly weakened at high doping level. It is clear that refractive index and extinction coefficient are closely correlated with crystalline size for undoped films, whereas it turns to the doping level for doped films, which can be performed by the mechanism of indium atom substitution. This work provides a very useful guild for design and application of optical–electronic devices.

1 Introduction

Cadmium oxide (CdO), well known as one of the transparent conductive oxides (TCOs), has been receiving tremendous attention over the past several decades due to the high electrical conductivity ($\sim 10^{-3} \Omega/\text{cm}$) and optical transmittance in the visible infrared region [1–3]. They are widely considered as promising candidate materials in optoelectronic fields, including gas sensor [4–6], photovoltaic cell devices [7, 8] combing with other interesting materials [9–11], phototransistors [8], IR detectors, and antireflection coatings [12].

Unfortunately, there are intrinsic limitations hindering the successful application of CdO films including the small band gap and low transmittance, especially in the short wavelength range. Increasing efforts have been devoted to solve these problems with the aim to improve the electrical as well as optical properties of TCOs. Until now, alien elements (fluorine (F) [13], aluminum (Al) [14], titanium (Ti) [15], indium (In) [16, 17], tin (Sn) [18], samarium (Sm) [19], iron (Fe) [20], etc.) doping in CdO film present a robust approach to improve the performance. Among the various elements, In-doped CdO (ICO) films are generally regarded as the most suitable candidate [21, 22] due to the similarity between In and Cd, donating role and superior properties. However, most researchers largely limited their focus on the electrical conductivity, transmittance, and band gap [23–26]. The optical constants, refractive index, and extinction coefficient are the fundamental and key parameters in optical and electric applications. The designing and optimizing photovoltaic devices and solar cell structures await urgent study on optical constants, such as refractive index and extinction coefficient. Unfortunately, previous work did not fully uncover these points.

Yuankun Zhu and Pei Lei have contributed equally to this study.

✉ Yuankun Zhu
zhuyuankun@usst.edu.cn

✉ Pei Lei
leipei.1232008@163.com

¹ School of Materials Science and Engineering, University of Shanghai for Science and Technology, Shanghai 200093, People's Republic of China

² Center for Composite Materials, Harbin Institute of Technology, P. O. Box 3010, Yikuang Street 2, Harbin 150080, People's Republic of China

In the present work, the influences of In doping and annealing on microstructure and optical constants of CdO films were studied. The chemical bonds, crystal structure, and morphologies of films at both different doping levels and gas annealing processes were characterized. Building the direct relation between the treatment conditions and optical constants is fundamentally and technologically needed for application.

2 Experimental details

A series of ICO films were grown on borosilicate glass by pulsed filtered cathodic arc deposition (PFCAD). Separate cadmium and indium metal pallets were used as Cd and In source, respectively, and the In and Cd ratio was adjusted alternatively by pulses of two sources. The plasma sources were two “miniguns” with rod cathodes of 6.25 mm diameter. Each cathode was enclosed by an alumina ceramic tube such that the cathode spots can operate only on the front surface [25]. The plasma stream passed a 90°-bent open filter to remove most of the macroparticles. The process gas composition was monitored by a differentially pumped quadrupole mass spectrometer (model RGA100 by SRS). The combination of flow and pumping speed resulted in a total pressure monitored by a Baratron® capacitance manometer. Oxygen was introduced into chamber as the reactive gas. The substrate temperature was maintained at 230 °C, and the oxygen pressure was kept at 7 mTorr, which is the optimized oxygen pressure according to the previous research; more details can be found in somewhere [25]. The thickness of all films was around 230 nm. Afterward, all the films were annealed in air and nitrogen atmospheres and kept at 450 °C for 1 h, then naturally cooled down to room temperature.

The film thickness was evaluated by profilometry with an accuracy of ± 10 nm. The element concentration of films was determined by EDS and XPS, and the In atomic concentration in CdO films varied from 0 to 9.1 %. High-resolution XPS (PHI 5700ESCA) was employed to determine the chemical bonds. The XPS apparatus was performed using a monochromatized Al K α X-ray source (radiation at 1486.6 eV) in an ultrahigh vacuum chamber. Film crystal structure was characterized by XRD, which is equipped with an area detector or a Phillips X’Pert-Pro X-ray diffractometer. Surface morphology was studied with a Veeco MultiMode AFM (Veeco, Plainview, NY) in tapping mode. Optical properties, such as refractive index and extinction coefficient, were characterized by spectroscopic ellipsometer (alpha-SE, J.A. Woollam) in the range from 380 to 900 nm. The incident angle was set 70° when collecting the data.

3 Discussion and results

In concentrations (In:Cd, at.%) of ICO films were measured as 0, 2.4, 4.2, and 9.1 % by EDS in the previous work [25]. In order to explore the chemical bonds, XPS was employed to scan the core levels. Figure 1 shows the XPS spectra of typical ICO film with In concentration of 9.1 %. Figure 1a shows the XPS survey spectra for the surface of CdO and In:CdO (9.1 %) films. It is clear to observe that obvious In peaks are from In:CdO film, and no In signals come from pure CdO film. Other elements are Cd, O, and C, indicating the high purity of films. Figure 1b shows the Cd3d core-level spectra. Using the optimal proportion of Gaussian to Lorentzian lineshape, the Cd3d line shape can be deconvoluted into two peaks at around 404.8 eV and 411.6 eV, which is consistent with the Cd–O bond of CdO [27]. In3d core-level spectrum is shown in Fig. 1c; similarly, In3d signal shows the two splitting peaks due to the spin–orbit coupling. The two peaks are located at around 444.4 eV and 452.1 eV, which is consistent with the peak position from ITO [28]. It is interesting to note that there is no pure metal In peak (~ 443.8 eV), indicating all the In atoms form the oxidation state. Figure 1d shows the O 1s core-level spectra and the fitting results. The spectra can be deconvoluted into three peaks at 529.5, 530.2, and 531.6 eV, respectively, corresponding to O–Cd bond, O–In bond, and physisorbed oxygen [29], which are generally observed in oxide films. Therefore, the results show that In atom could form O–In bond in the Cd–O matrix instead of In–In bond.

Figure 2 shows the XRD plots of CdO films with different In doping concentrations for as-grown, annealed-in-air, and nitrogen samples, respectively. All the films show pure fcc structure of CdO (PDF card No: 005-0640) with polycrystalline phase. Pure CdO film shows the preferred (111) orientation, which is consistent with the previous reports [30, 31]. With the increase of In doping, the preferential orientation transforms into (200) orientation, and the intensity of (222) gradually reduces to the weakest one until ICO film with 9.1 % concentration. Since (200) direction has a lower surface energy than (111) direction [32], it indicates that In doping could promote the preferential (111) crystalline growth due to the change of internal stress and growth rate [17], and the similar phenomena were also observed in F:CdO films [33]. In doping does not change phase structure even at high concentration. According to the previous discussion, it is reasonable that the In atom substitutes the Cd atom in the CdO lattice. The phase structure remains same phase and preferred orientation regardless of annealing in nitrogen and air at 450 °C, indicating the super phase stability.

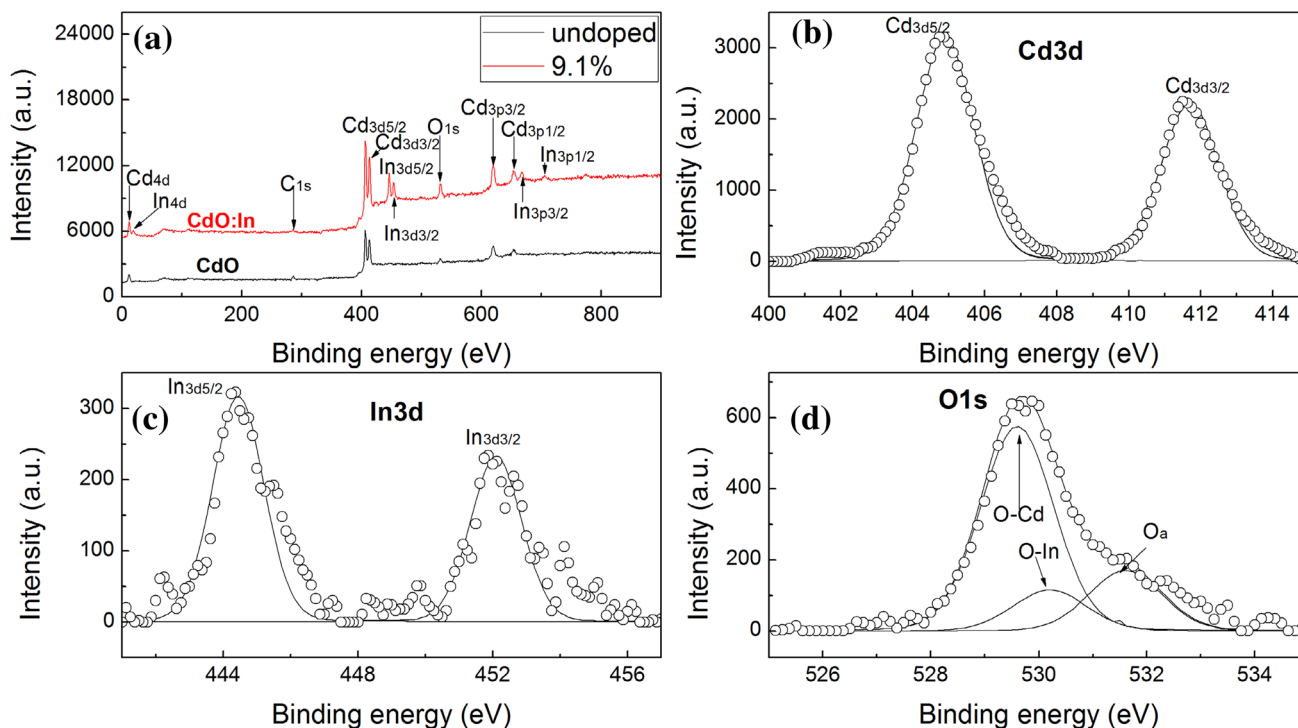


Fig. 1 a XPS survey spectra of In-undoped and In-doped CdO films with In concentration of 9.1 %, the **b** Cd3d, **c** In3d, and **d** O 1s core-level spectra of ICO films with In concentration of 9.1 %

In order to evaluate the film crystallinity, the crystalline size was evaluated by Scherrer's equation using the full width at half maximum (FWHM) of the strongest peaks. Figure 3 shows that the crystalline size changes with indium doping and annealing process. It is clear that In doping could prohibit the crystalline growth and form small crystallines, which is similar to Ga doping in CdO films [34], but is contrary to Tl doping in CdO films [35]. Note that the crystalline size drops within a small range as the doping varies from 0 to 9.1 %. Under gas annealing, with the increase of In doping, crystalline still shows smaller size regardless of nitrogen and air, whereas the annealed ICO films show larger crystallines compared with the as-deposited samples. The high temperature promotes the larger crystallines of CdO under the 400 °C annealing due to the coarsening role [30, 36]. The refinement role In doping plays works in both the as-grown and annealed samples.

The surface morphology of ICO films is shown in Fig. 4. Under nitrogen and air annealing, the influence of In doping on the surface roughness is similar to the influence of In doping in the as-grown CdO films [25], and more In doping induces more smooth surface. However, annealing procedure promotes rough surface at low In doping level,

and this role disappears at high doping levels. The large roughness is attributed to the large crystal crystallines under annealing; in contrast, high In doping causes small crystalline and also flat surface morphology.

Optical properties of ICO films, including refractive index (n) and extinction coefficient (k), were measured by SE at room temperature. In order to extract the accurate n and k values, three-layer model (EMA/CdO:In/glass substrate) was built as shown in Fig. 5a. Under considering the transparency in the whole range (380–900 nm) and slight absorption near the 380 nm, Cauchy–Urbach dispersive model was selected for ICO films [37]. The good fitting results between the model and measured Psi and Delta were obtained, indicating the optimal model and measured results as shown in Fig. 5b.

The optical constants, such as refractive index and extinction coefficient, can be tainted according to the fitting results. Figure 6a shows the refractive index of ICO films as the doping concentration increases from 0 to 9.1 %. Both n and k increase as the wavelength decreases due to approaching the bandgap. Without In doping, the film shows high n value (2.52 at 500 nm). It gradually reduces into the low value (2.28 at 500 nm) when it reaches 9.1 % doping. Extinction coefficient can also be adjusted by In

Fig. 2 XRD patterns of ICO films grown at 230 °C and 7 mTorr with different In concentrations

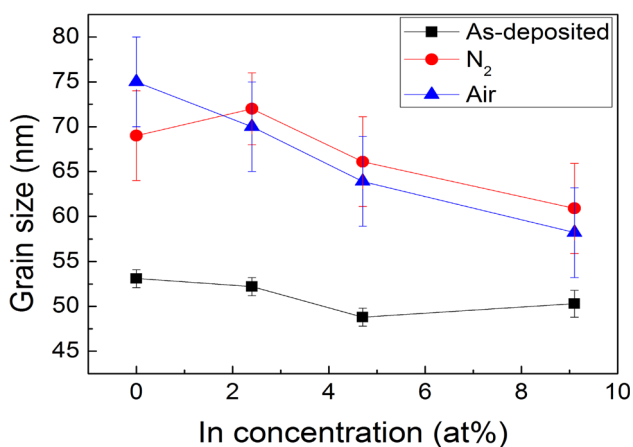
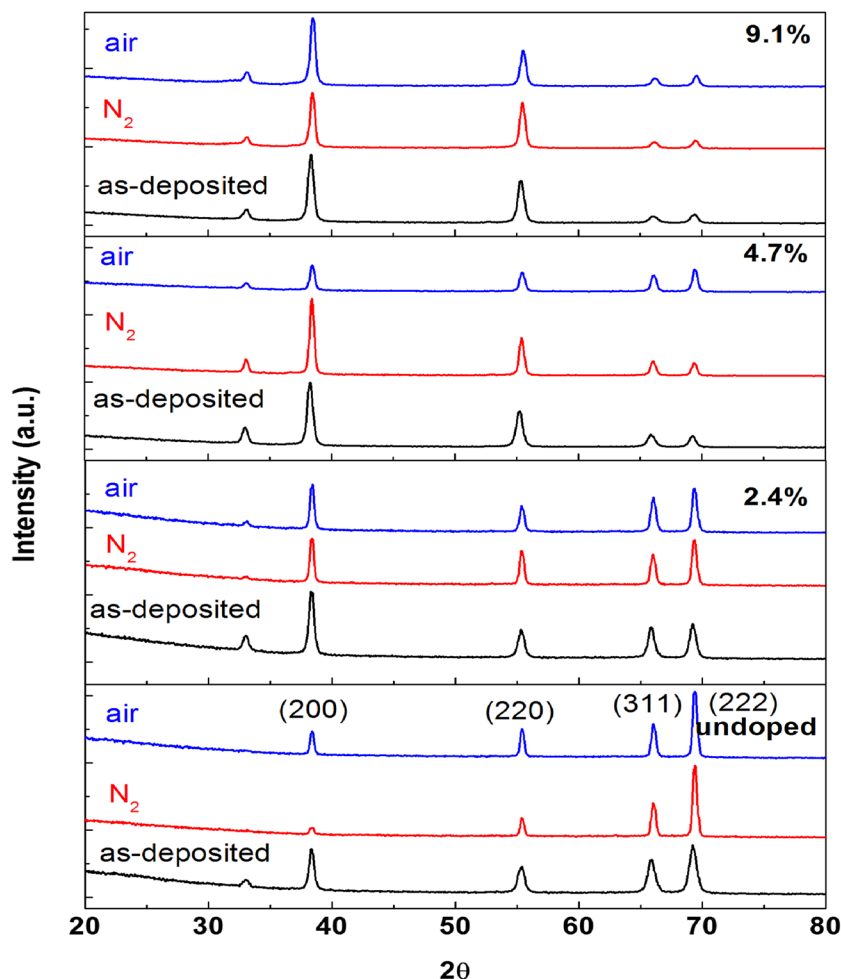


Fig. 3 Crystalline size of ICO films: **a** as-deposited; **b** annealing in nitrogen; **c** annealing in air at different In concentrations

doping. For comparison, the refractive index and extinction coefficient of commercial ITO films (Filmetrics Company) are 1.972 and 0.043 at 500 nm, respectively. Without In doping, the film shows k abruptly increases to high value in

the range of less than 450 nm. This trend can be relieved by In doping in the films. The shrink of absorption with the increase of In doping concentration is attributed to the enlarged bandgap [25]. Naturally, the refractive index is closely linked to the crystallinity. As shown in Fig. 3, the crystalline size gradually reduces with the increase of In doping concentration. More In doping concentration means smaller crystallines; more grain boundaries contain more pores and holes deciding the low n .

The influences of annealing on n and k were studied in nitrogen and air atmosphere in Fig. 7. It is clear that nitrogen and gas annealing play the similar role. Without In doping, the annealed ICO films show higher n value than the as-deposited ones. Annealing could promote large crystalline and have high density. However, when doping In element, n value abruptly drops below as-grown one. The crystalline size of annealed ICO films is still larger than that of as-grown film. The annealed ICO films with larger crystallines have small refractive index, which is mainly attributed to the substitution of In atoms in the Cd lattice positions. The more substitution of In, the lower

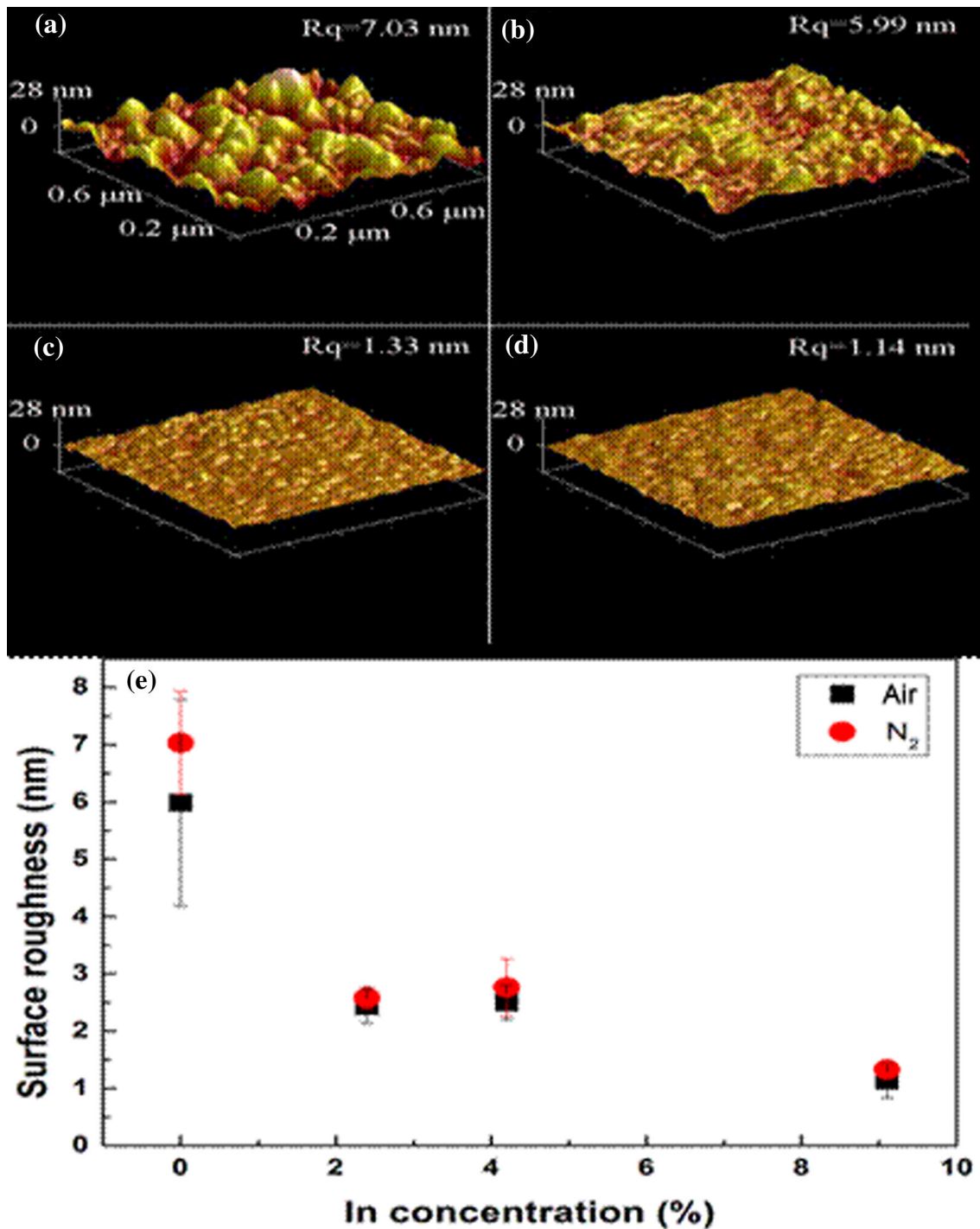


Fig. 4 Surface morphologies of ICO films under annealing: **a, b** undoped; **c, d** 9.1 % In doping; **a, c** nitrogen annealing; **b, d** air annealing; **e** surface roughness of ICO films with different In concentrations in nitrogen and air annealing

refractive index it has as the low n of In_2O_3 compared with n of CdO [38, 39]. It is reasonable to observe that ICO films have lower refractive index even after annealing process. In doping could reduce the extinction coefficient with the high doping level, which can be adjusted in a small extent by nitrogen and air annealing treatment.

4 Conclusion

ICO films with different In concentrations were prepared to study the influence of doping level and annealing on structural and optical properties in detail. The indium atom forms chemical bonds in Cd–O matrix instead of metallic

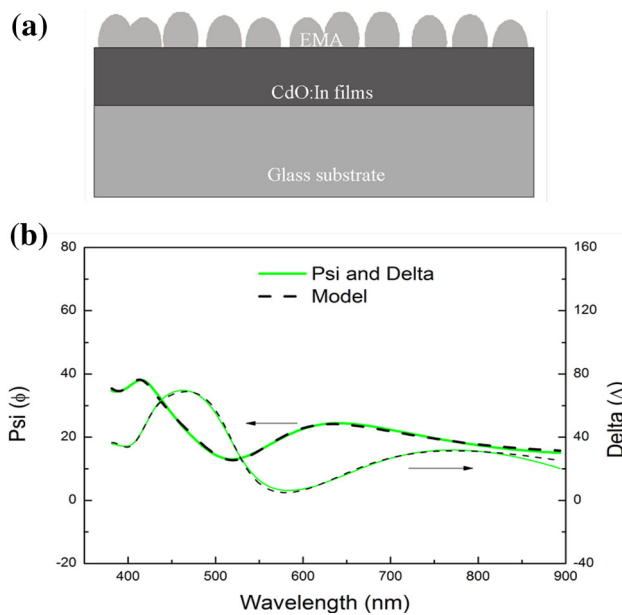


Fig. 5 **a** The 3-layer built model; **b** the fitting results between the model and measured data

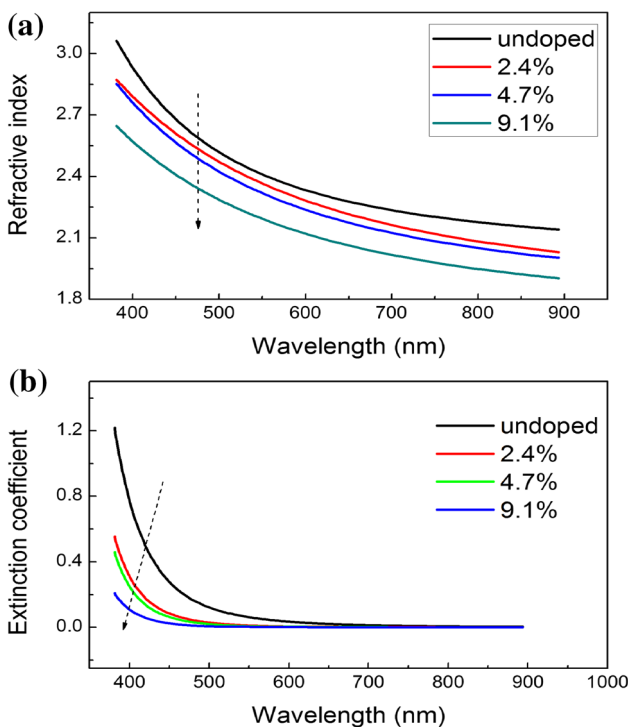


Fig. 6 The variation of **a** refractive index and **b** extinction coefficient of ICO films as a function of In doping concentration

In–In bonds. Indium doping maintains the cubic phase, but it transforms the preferential (222) orientation into (200) one. Annealing coarsens the large crystallines of ICO films compared with these of the as-grown film. The undoped CdO film shows high refractive index of 2.52 at 500 nm,

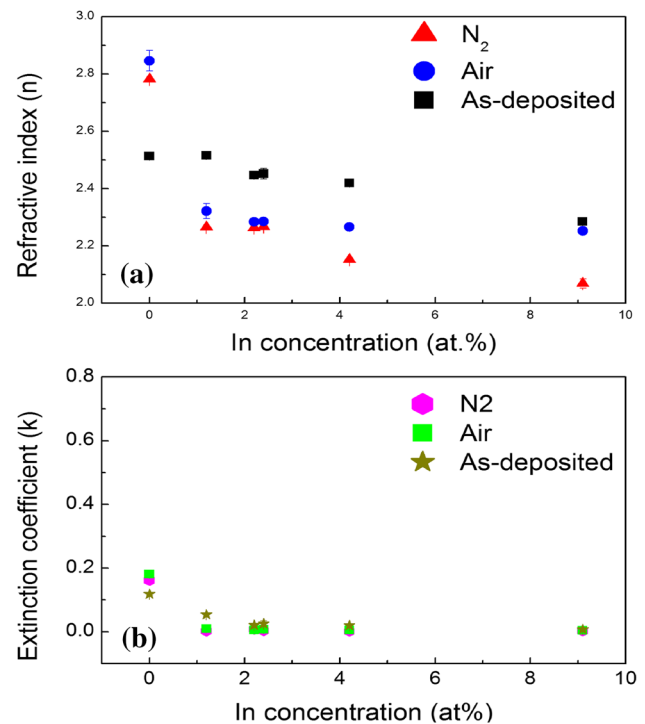


Fig. 7 **a** Refractive index and **b** extinction coefficient of ICO films with different In concentrations in nitrogen and air annealing

while the low value of 2.28 at 500 nm is achieved when it reaches 9.1 % doping. Refractive index of undoped films can be enhanced through annealing process due to the large crystalline. The way of In doping could reduce the refractive and extinction coefficient and stabilize them even under annealing process. Low refractive index of about 2.1 is obtained for CdO films annealed in nitrogen. The work is critical for the design and application of optical–electronic devices.

Acknowledgments The authors would like to thank Doctor Andre Anders from Lawrence Berkeley National Laboratory for the help of sample preparation. The authors thank the National Natural Science Foundation of China (No. 11402149), Natural Science Foundation of Shanghai (14ZR1428000), and the Hujiang Foundation of China (B14006) for the financial support of this research.

References

1. P.H. Jefferson, S. Hatfield, T.D. Veal, P. King, C.F. McConville, J. Zúñiga-Pérez, V. Muñoz-Sanjósé, *Appl. Phys. Lett.* **92**, 022101 (2008)
2. M. Yan, M. Lane, C. Kannewurf, R. Chang, *Appl. Phys. Lett.* **78**, 2342 (2001)
3. E. Sachet, C.T. Shelton, J.S. Harris, B.E. Gaddy, D.L. Irving, S. Curtarolo, B.F. Donovan, P.E. Hopkins, P.A. Sharma, A.L. Sharma, *Nat. Mater.* **14**, 414 (2015)
4. R. Salunkhe, C. Lokhande, *Sens. Actuators B: Chem.* **129**, 345 (2008)

5. A. Kamble, R. Pawar, N. Tarwal, L. More, P. Patil, *Mater. Lett.* **65**, 1488 (2011)
6. R. Bulakhe, C. Lokhande, *Sens. Actuators B: Chem.* **200**, 245 (2014)
7. R. Call, N. Jaber, K. Seshan, J. Whyte, *Sol. Energy Mater.* **2**, 373 (1980)
8. E. Fortunato, D. Ginley, H. Hosono, D.C. Paine, *MRS Bull.* **32**, 242 (2007)
9. D. Pathak, T. Wagner, T. Adhikari, J.M. Nunzi, *Synth. Met.* **199**, 87 (2015)
10. D. Pathak, R.K. Bedi, D. Kaur, *Optoelectron. Adv. Mater.* **4**, 675 (2010)
11. D. Pathak, R.K. Bedi, D. Kaur, R. Kumar, *Chalcogenide Lett.* **8**, 213 (2011)
12. A. Kaźmierczak-Bałata, J. Bodzenta, D. Korte-Kobylińska, J. Mazur, K. Gołaszewska, E. Kamińska, A. Piotrowska, *Appl. Optics* **48**, C74 (2009)
13. I. Akyuz, S. Kose, E. Ketenci, V. Bilgin, F. Atay, *J. Alloy. Compd.* **509**, 1947 (2011)
14. R. Maity, K. Chattopadhyay, *Sol. Energy Mater. Sol. Cells* **90**, 597 (2006)
15. R. Gupta, K. Ghosh, R. Patel, P. Kahol, *Appl. Surf. Sci.* **255**, 6252 (2009)
16. S. Kose, F. Atay, V. Bilgin, I. Akyuz, *Int. J. Hydrog. Energy* **34**, 5260 (2009)
17. B. Zheng, J. Lian, L. Zhao, Q. Jiang, *Appl. Surf. Sci.* **256**, 2910 (2010)
18. Z. Zhao, D. Morel, C. Ferekides, *Thin Solid Films* **413**, 203 (2002)
19. A. Dakhel, *J. Alloy. Compd.* **475**, 51 (2009)
20. A. Dakhel, *Thin Solid Films* **518**, 1712 (2010)
21. H. Kawazoe, K. Ueda, *J. Am. Ceram. Soc.* **82**, 3330 (1999)
22. D. Kammler, T. Mason, D. Young, T. Coutts, D. Ko, K. Poepelmeier, D. Williamson, *J. Appl. Phys.* **90**, 5979 (2001)
23. S. Jin, Y. Yang, J.E. Medvedeva, L. Wang, S. Li, N. Cortes, J.R. Ireland, A.W. Metz, J. Ni, M.C. Hersam, *Chem. Mat.* **20**, 220 (2007)
24. R. Gupta, K. Ghosh, R. Patel, S. Mishra, P. Kahol, *Mater. Lett.* **62**, 3373 (2008)
25. Y. Zhu, R.J. Mendelsberg, J. Zhu, J. Han, A. Anders, *Appl. Surf. Sci.* **265**, 738 (2013)
26. S. Ghosh, S. Neogi, P. Biswas, *Mater. Res. Express* **1**, 045201 (2014)
27. A. Gulino, P. Dapporto, P. Rossi, I. Fragala, *Chem. Mat.* **14**, 4955 (2002)
28. H. Kato, S. Takemura, Y. Nakajima, *J. Appl. Phys.* **81**, 7313 (1997)
29. T. Subramanyam, G.M. Rao, S. Uthanna, *Mater. Chem. Phys.* **69**, 133 (2001)
30. S. Aksoy, Y. Caglar, S. Ilican, M. Caglar, *Int. J. Hydrog. Energy* **34**, 5191 (2009)
31. F. Eze, *Mater. Chem. Phys.* **89**, 205 (2005)
32. D. Ma, Z. Ye, L. Wang, J. Huang, B. Zhao, *Mater. Lett.* **58**, 128 (2004)
33. M. Kul, A.S. Aybek, E. Turan, M. Zor, S. Irmak, *Sol. Energy Mater. Sol. Cells* **91**, 1927 (2007)
34. R. Deokate, S. Salunkhe, G. Agawane, B. Pawar, S. Pawar, K. Rajpure, A. Moholkar, J. Kim, *J. Alloy. Compd.* **496**, 357 (2010)
35. A. Dakhel, *Phys. Status Solidi A* **205**, 2704 (2008)
36. J. Santos-Cruz, G. Torres-Delgado, R. Castanedo-Perez, S. Jiménez-Sandoval, O. Jiménez-Sandoval, C. Zuniga-Romero, J.M. Marín, O. Zelaya-Angel, *Thin Solid Films* **493**, 83 (2005)
37. K. Siraj, M. Khaleeq-ur-Rahman, S. Hussain, M. Rafique, S. Anjum, *J. Alloy. Compd.* **509**, 6756 (2011)
38. F.O. Adurodija, L. Semple, R. Brüning, *J. Mater. Sci.* **41**, 7096 (2006)
39. R. Reddy, Y.N. Ahammed, K.R. Gopal, D. Raghuram, *Opt. Mater.* **10**, 95 (1998)